Potential Impacts of Sand Mining Offshore of Maryland and Delaware: Part 1—Impacts on Physical Oceanographic Processes

Jerome P.-Y. Maa†, Carl H. Hobbs, III†, S.C. Kim‡, and Eugene Wei§

†Virginia Institute of Marine Science
College of William and Mary
Gloucester Point, VA 23062, USA

‡Environmental Laboratory ERDC
Corps of Engineers, US Army
Vicksburg, MS 39180, USA

§National Ocean Service NOAA
Silver Spring, MD 20910, USA

ABSTRACT

MAA, J.P.-Y.; HOBBS, III, C.H.; KIM, S.C., and WEI, E., 2004. Potential impacts of sand mining offshore of Maryland and Delaware: part 1—impacts on physical oceanographic processes. *Journal of Coastal Research,* 20(1), 44–60. West Palm Beach (Florida), ISSN 0749-0208.

In an effort to assess the possible changes to physical oceanographic processes that might result from alteration of bathymetry as a result of dredging or sand mining, we evaluated the differences in the output of various numerical models run with the natural and hypothetical post-dredging bottom conditions. Fenwick and Isle of Wight Shoals offshore of the Delaware-Maryland border of the mid-Atlantic continental shelf served as the test site. We considered two dredging scenarios, a one-time removal of 2×10^6 m³ of sand from each of two shoals and a cumulative removal of 24.4×10^6 m³, but only the larger appeared significant.

The study of wave transformation processes relied upon a series of runs of the REF/DIF-1 model using sixty wave conditions selected from analysis of the records from a nearby, offshore wave gauge. The model was tuned and calibrated by comparing measured near-shore wave conditions with data calculated using the same measured offshore waves that generated the real near-shore conditions. The modeled, post-dredging data indicated an increase in wave height of up to a factor of two in the area between the dredged shoals and the shore and, in some locations, a lesser increase in breaking wave height and a decrease in breaking wave height modulation. The model results also may help explain the existing pattern of erosion and relative stability.

Application of the well-known SLOSH model (Sea, Lake, and Overland Surges from Hurricanes) for storm surge and POM (Princeton Ocean Model) for tidal currents indicates that the likely dredging related changes in those processes are negligible.

ADDITIONAL INDEX WORDS: *Dredging, wave transformation, tidal current, storm surge, shoreline responses, numerical simulation.*

INTRODUCTION

A well maintained beach can serve several purposes, *e.g.,* (1) reducing the rate of land loss, (2) providing a public recreational area, and (3) protecting valuable properties and infrastructure that are located near the coastline. Thus, a great deal of effort has been devoted to understanding the physical processes on the adjacent beach that might be changed by offshore sand mining. Among all possible physical processes, the following three may have a direct influence: waves that reach the coastline; local tidal currents; and storm surges that are responsible for raising the water level. The possible impacts on biological processes at the sand mining sites and beach nourishment sites were reported separately as part 2 in this JCR volume.

One can use several approaches, either separately or in combination, to protect an eroding beach. In the coastal sector near the Maryland–Delaware border, especially around Ocean City, Maryland, the beach has been nourished throughout the past two decades. It has become increasingly difficult to find terrestrial sources of good, beach-quality sand. Near shore submarine sources are limited and problematical. The continual loss of sand to shore normal and along-shore transport processes requires a reliable source of good quality sand for future nourishment.

Two offshore shoals, Fenwick Shoal and Isle of Wight Shoal (Figure 1), have been identified as potential sources for beach-quality sand (CUTTER *et al.,* 2000; HOBBS, 2002). Fenwick Shoal is approximately 10 km west of the Maryland–Delaware border. Isle of Wight Shoal is about 8 km south of Fenwick. There is concern that utilization of sand from these shoals may cause unwanted alterations to the shoreline, which may be near its dynamic equilibrium state. Sand mining at these two shoals definitely will alter the wave transformation processes which, depending upon the mining plan, may induce unfavorable consequences.

Understanding the possible changes in the shoreline resulting from dredging requires a comprehensive understanding of the wave climate, the wave transformation processes, the possible changes of wave transformation caused by changing the bathymetry, and the associated shoreline responses.
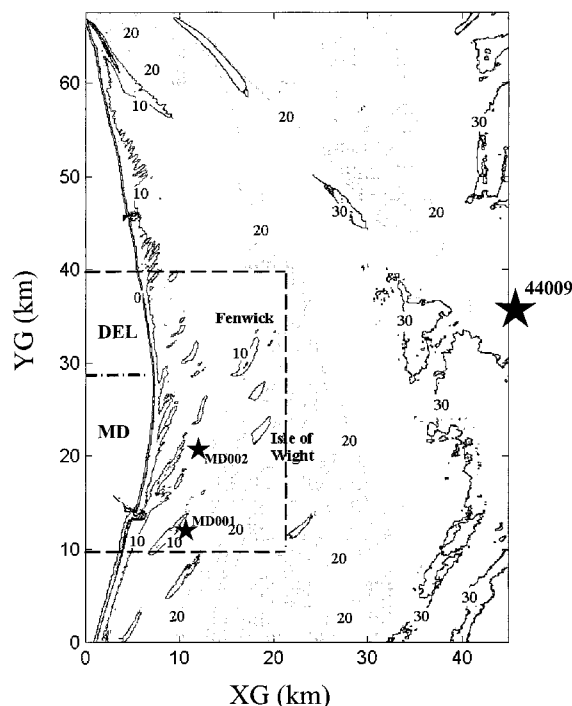
Figure 1. Bathymetrical contours (meter) of the entire computation domain. The computing results will be displayed for a much smaller display domain marked by the dashed lines. The relative locations of wave station 44009, MD001, MD002 are also marked.

In a study of a similar problem at Sandbridge Shoal, Virginia, MAA and HOBBS (1998) concluded that if sand taken from the shoal were limited on the order of 10^6 m³, the impact on wave transformation would cause a less-than-five-percent change of local breaking wave height for the most severe sea condition (wave height = 6.2 m, period = 20 s) applied at the offshore. The five percent change is not significant because the change was determined using a wave transformation model (RCPWAVE) that is known to overestimate wave height near shore (MAA et al., 2000). Thus, the actual change might be negligible small considering the overall accuracy of offshore wave conditions (i.e., 5% in wave height, 1 second in wave period, and ± 5 degrees in wave direction, MEINDL and HAMILTON, 1992).

The foci of the present study are (1) determining if the possible impact resulting from a one-time sand mining event on the order of 2×10^6 m³ of sand at each of the two shoals is acceptable and (2) estimating the possible alterations to waves resulting from removal of significantly more sand, on the order of 10^7 m³.

In order to estimate the possible impact, a computational bathymetric grid system was established first, followed by a study of wave climate in this area. Wave data measured at offshore station 44009 (from 1986–1998) were used (Figure 1). Sixty wave conditions were selected to cover the majority of possible wave conditions that would be affected by altering the bathymetric condition, and the REF/DIF-1 wave transformation model was used to check the original wave height

distribution in this study domain. For the one-time sand mining, we found that the possible change of wave transformation is negligibly small. Thus, further discussion of this scenario is omitted in this paper.

To find the possible impact of cumulative sand mining at the two sites, the same 60 offshore wave conditions were re-run with bathymetry altered to provide a total of 24.4×10^6 m³ sand. Details on the modeled sand mining plan and the results on changing waves are given in this paper.

In addition to the analysis of the possible changes in wave transformation resulting from sand mining, possible changes to tidal currents and storm surge were also checked. By applying the suite of tidal constituents determined by analyzing a year long record obtained at Ocean City, Maryland and the same sets of bathymetric data used in the wave transformation studies to the Princeton Ocean Model (BLUMBERG and MELLOR, 1987), the possible alterations for tidal currents at maximum flood and ebb were identified. Similarly paired runs of the SLOSH (Sea, Lake, and Overland Surges from Hurricanes) model (JELENIANSKI et al., 1992) provided information on the possible alterations to storm surge.

BATHYMETRY

Bathymetric data sorted into one degree latitude-longitude domains were obtained from the NOAA Data Center. The data and the retrieving software were both provided on CD-ROM. An arbitrary and sufficiently large domain about 80 km in the east-west direction and about 100 km in the north-south direction was used for bathymetry data retrieval. The original coordinates of the data were latitude and longitude, which were transferred to the Maryland State Plane Coordinate System using the CORPSCON software from the Waterways Experiment Station, U.S. Army Corps of Engineers. Bathymetric data for inland waterways were removed, and a computing grid of 44.970 Km and 67.560 km (Figure 1) with uniform cell size (30 meters in XG-direction and 60 m in YG direction) was generated, where XG and YG stand for the X and Y direction of the computing Grid. Thus, the computing grid has 1500 and 1127 grid points in the XG and YG directions, respectively. The small cell size is needed for simulation of wave diffraction. The large computational domain is necessary to minimize the possible inaccurate boundary effects specified at the lateral boundaries for wave transformation simulation. For displaying the computation results, however, a much smaller domain (hereafter called the display domain) marked as the dashed line in Figure 1 is sufficient.

The coordinates of the origin of this computational grid are E561.000 km and N61.000 km in NAD83 Maryland State Plane Coordinate System, and YG is rotated 4.2 degrees from the Maryland State Plane Coordinates' North coordinate.

Two mining areas were selected at the two shoals (Figure 2 and Table 1) with a possible maximum sand removal of 24.4 $\times 10^6$ m³ if a constant dredging depth of three meters is selected. This scenario represents a possible cumulative sand removal from the two shoals over 10 to 20 years. The selection of these two mining areas was arbitrary and was based on the geometry. It is suggested that it would be better to
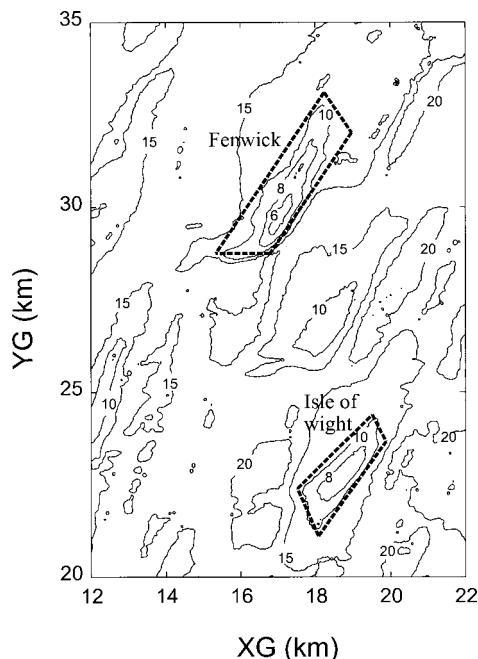
Figure 2. Detailed bathymetric contours (meter) at the vicinity of Fenwick and Isle of Wight Shoals. The modeled areas for sand mining for a total of 24 × 10⁶ m³ are marked as dashed polygons, and the coordinates are given in Table 1.

flatten a shoal rather than to create a depression on an otherwise flat area.

WAVE DATA

The National Data Buoy Center (NDBC) has a moored buoy station, 44009 (Lat. 38°27′49″ N, Long. 74°42′07″ W), located about 40 km offshore of the Ocean City at a water depth of 28 m. This station has collected non-directional wave spectrum information since May 1986 and directional wave spectrum information since 1993. All processed data were archived at the National Oceanic Data Center (NODC) in Washington, D.C. Because of the site's proximity (Figure 1), these wave data are used directly in this study.

Near shore, the U.S. Army Corps of Engineers had one wave station (MD001, Figure 1), north of Ocean City, Maryland (Lat. 38°24′00″ N, Long. 75°30′00″ W) from Oct. 1993 to Jan. 1998. The Corps also has another station, MD002 (Lat. 38°20′24″ N and Long. 75°04′12″ W), south of Ocean City. The water depth is 9 m at both stations. Wave measurements at these two near shore stations are directional wave distributions.

In this study, wave data at the two near shore stations are used for verifying the accuracy of calculated wave heights using the wave information (significant wave height, peak wave period, and peak wave direction) specified at the offshore boundary where station 44009 is located. For example, wave records from Nov. 1 to Nov. 30, 1997 at both stations 44009 and MD001 (Figure 3) show the differences in wave conditions between these two stations. For this period, the

Table 1. *Coordinates of the marked points for the modeled cumulative sand mining (in Maryland State Plane Coordinates, NAD83, meters).*

Item	Fenwick Shoal	Isle of Wight Shoal
Area	5.36 × 10⁶ M²	2.82 × 10⁶ M²
Volume	16 × 10⁶ M³	8.4 × 10⁶ M³
E (m)	578,406.0000	580,071.0630
N (m)	88,298.5469	81,889.3906
E (m)	581,607.3750	582,308.5630
N (m)	92,705.9219	83,820.7109
E (m)	582,123.0000	582,634.3130
N (m)	91,535.0156	83,205.1953
E (m)	579,939.2500	580,428.6250
N (m)	88,286.2266	80,750.1406

wave conditions are almost the same for MD001 and MD002. Notice that in this period the offshore wave height varies from less than 0.5 m to 5 m, which is a sufficient range for calibrating the wave transformation model selected.

Wave Statistical Analysis

The joint distribution of significant wave height and peak energy wave period for station 44009 reveal that the most frequently occurring wave has a period of 9 seconds and significant wave height of 0.6 meters. Wave height greater than 6 m is rare, occurring only a few times during the entire 13 years of observation (1986–1998) with a total duration of 46 hours which is about 0.04 percent of the record.

The available directional wave data (1993–1997) indicates that waves mainly come from the following 7 directions: SSE, SE, ESE, E, ENE, NE, and NNE (Figures 4 and 5). A few large waves came from NNW and NW, but were ignored in this study because they travel offshore away from the area of interest.

Assuming the available wave directional information represents the true wave direction distribution, we can regroup
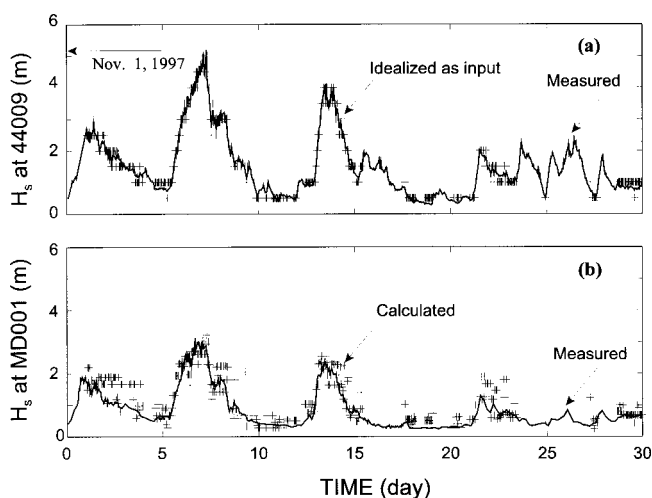

Figure 3. Verification of REF/DIF-1 wave transformation model. (a) The measured and specified idealized input wave conditions at station 44009, (b) The measured and calculated wave heights at MD001.
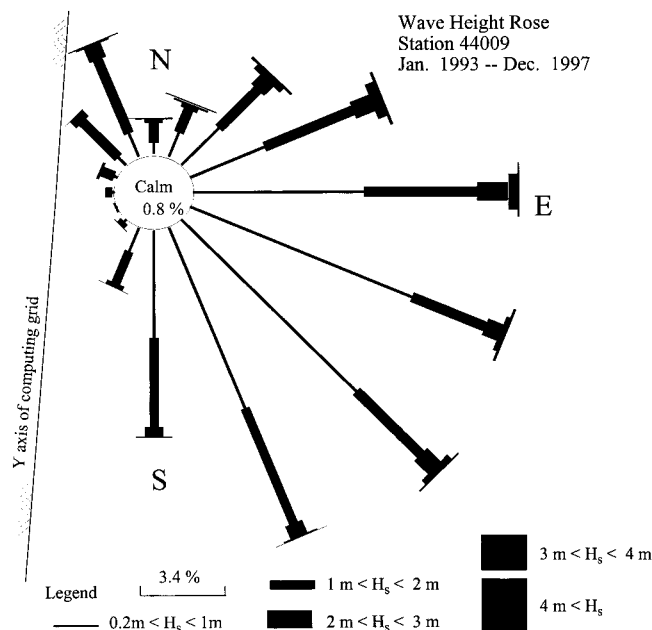
Wave Height Rose
Station 44009
Jan. 1993 -- Dec. 1997

Legend

3.4 %

0.2m < H$_s$ < 1m

1 m < H$_s$ < 2 m

2 m < H$_s$ < 3 m

3 m < H$_s$ < 4 m

4 m < H$_s$

Figure 4. Significant wave height rose at station 44009. The scale of 3.4% occurrence is plotted in the legend.

Wave Period Rose
Station 44009
Jan. 1993 -- Dec. 1997

Legend 7.3 %

5 s < T < 8 s
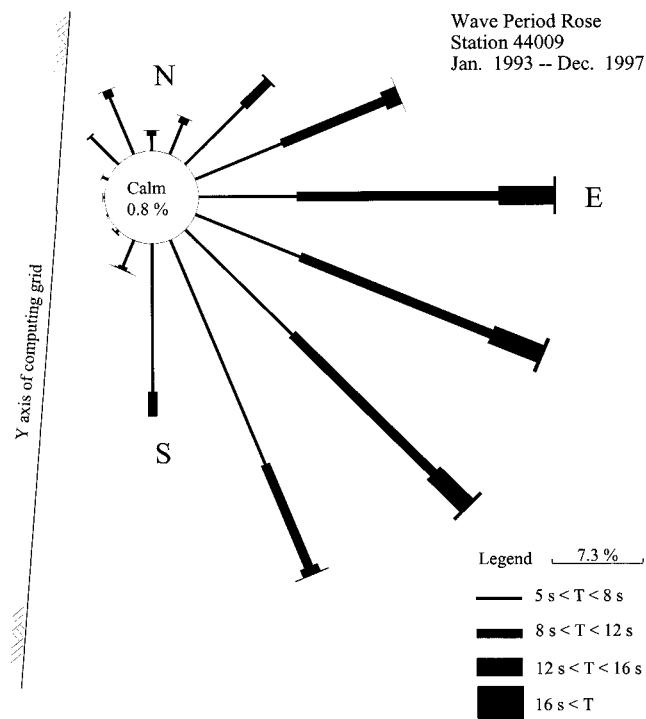
8 s < T < 12 s

12 s < T < 16 s

16 s < T

Figure 5. Peak energy wave period rose at station 44009. The scale of 7.3% occurrence is plotted in the legend.

the waves into bins for analyses. For practical and feasible computational purposes, we sorted wave height from 0.25 to 8 m with an interval of 0.5 m, wave period from 3 to 20 s at an interval of 2 s, and wave direction into 16 major directions. Using the above conditions for sorting, the joint probability distribution of wave height and period that occurred for the ENE direction is given in Table 2 as an example. Notice that wave conditions in the four major directions (ENE, E, ESE, SE) counted for more than 50 percent of all wave conditions, and only from the SE direction, wave period has reached 20 seconds.

Wave Height

Table 3 shows the annual maximum significant wave heights (H$_s$) that were observed at station 44009 from 1986

to 1998. The recorded maximum significant wave height (7.6 m with a peak wave period of 16.7 seconds, occurred on 1/04/92) during the 13 observational years suggests that the possible most severe sea can be rounded for a significant wave height of 8 m and wave period of 20 s. Notice that among the observed maximum H$_s$, only one is possibly induced by a hurricane (August 16, 1995). The famous "Halloween Storm" (also know as "the Perfect Storm") happened in late October 1991 did not produce the largest H$_s$ in 1991.

Based on wave height, we suggested four categories (Table 4) of wave severity: The most severe sea (M) has a wave height of 8 m, severe sea (S) has a wave height of 6 m, rough

Table 2. *Height and period join distribution (in %) for waves coming from ENE (total 8.60%).*

H (m)	4s	6s	8s	10s	12s	14s	16s	>17s
0.5	0.1638	0.3545	0.3009	0.3515	0.3277	0.0596	0.0060	0
1.0	0.3128	0.9294	0.4737	0.5898	0.4975	0.0089	0.0	0
1.5	0.0834	0.5898	0.4290	0.5362	0.3634	0.0119	0.0	0
2.0	0	0.3426	0.3098	0.2800	0.1728	0.0149	0.0089	0
2.5	0	0.0715	0.1430	0.0983	0.0626	0.0119	0	0
3.0	0	0.0060	0.1370	0.1341	0.0626	0	0	0
3.5	0	0.0030	0.0715	0.0745	0.0387	0	0	0
4.0	0	0	0.0298	0.0298	0.0060	0	0	0
4.5	0	0	0.0030	0.0268	0.0030	0	0	0
5.0	0	0	0.0030	0.0060	0.0030	0	0	0
5.5	0	0	0	0.0030	0.0030	0	0	0
6.0	0	0	0	0.0119	0.0	0	0	0
6.5	0	0	0	0	0.0089	0	0	0
7.0	0	0	0	0	0.0030	0	0	0
Σ		2.1419	1.5522	0.1072	0.0149	0		

Table 3. *Observed annual maximum significant waves.*

Date	Time	H_Significant (m)	T_Peak (sec)
12/03/86	08:00	4.7	12.5
1/02/87	08:00	5.9	11.1
4/08/88	04:00	4.3	9.1
2/24/89	17:00	5.4	11.1
10/26/90	18:00	4.6	10.0
11/10/91	03:00	4.9	9.1
1/04/92	11:00	7.6	16.7
10/27/93	12:50	4.6	11.1
12/23/94	19:50	5.4	12.5
8/16/95	10:50	4.2	14.3
1/08/96	04:00	7.0	11.1
11/08/97	06:00	5.2	11.1
2/05/98	16:00	7.4	12.5

sea (R) has a wave height of 4 m, and Northeaster (N) has a wave height of 2 m.

Wave Direction

The available directional wave data indicate that large waves can come from the following seven directions: NNE, NE, ENE, E, ESE, SE, and SSE (Figure 4). Large waves coming from NNE to ENE are mainly caused by northeasters. Long period waves from these two directions, however, are relatively rare (Figure 5). Most of the waves from the NNE and NE are less than 8 sec. Long period waves mainly come from the ENE, E, ESE, and SE because of the long fetch. Thus, waves coming from ENE, E, ESE, and SE are selected as the important wave directions because of the possible long and large waves. Large and long waves coming from the SSE must be induced by hurricanes and the chance of this is relatively small, and thus, is not selected in this stage of study.

Model Waves

Based on the measurements at station 44009, we identified 60 wave conditions (Table 4) that included the above selected sea severities (M, S, R, G), five wave periods (10s, 12s, 14s, 16s and 20s), and four wave directions (ENE, E, ESE, and SE). Notice the 8 m wave height selected for the most severe sea would have much less impact if it comes with a short wave periods (*e.g.,* 12, and even 14 s) because they will be broken far away from coast, and thus, those short wave periods were excluded. Similarly, for the severe sea, wave periods of 10 s and 12 s are excluded. These 60 wave conditions can roughly represent the major wave components that should be modeled for possible changes due to the cumulative sand mining at the Fenwick Shoal and Isle of Wight Shoal. Short wave periods (less than 10 s) are excluded because the possible impact, if any, on these short period waves would be small. Our calculation results given in Figures 12 and 13, and Table 5 proved that the possible effect on breaking wave height is negligible when wave period is 10 s. We did not run a particular measured wave condition (for example, the most frequently occurring waves, T = 9 s, H = 0.5 m) because (1) the period is too short to be significantly affected by the modeled dredging, and (2) through checking the selected 60 wave

Table 4. *A selection of wave heights and periods for modeling.*

Wave Height (m)	Wave Period (s)
Most Severe Sea, 8	16, 20
Severe Sea, 6	14, 16, 20
Rough Sea, 4	10, 12, 14, 16, 20
Northeaster, 2	10, 12, 14, 16, 20

conditions, most of the waves that might be affected by dredging were considered. Because of the stochastic nature of waves, as well as the nonlinear process of energy dissipation caused by bottom friction, we should examine all possible wave conditions, and that is why 60 waves were selected to represent the entire wave field.

Selection of Wave Models

The many numerical models available for simulating water wave transformation can be divided into two categories: (1) Wave hindcast/prediction models (*e.g.,* SWAN, HISWAP, NSW in Mike 21, and STWAVE) and (2) Wave transformation models (*e.g.,* RCPWAVE, REF/DIF-1, REF/DIF-S, RIDE, and EMS module in Mike 21). Models in the first category are solving the generalized equation (Eq. 1) of wave spectral action density redistribution.

$$\frac{\partial N}{\partial t} + \frac{\partial c_x N}{\partial x} + \frac{\partial c_y N}{\partial y} + \frac{\partial c_\omega N}{\partial \omega} + \frac{\partial c_\theta N}{\partial \theta} = \frac{S}{\sigma} \qquad (1)$$

where $N(t, x, y, \omega, \theta) = E(t, x, y, \omega, \theta)/(\omega - Vt)$, E is energy density, ω is the absolute frequency, t is time, x and y are two horizontal directions, θ is spectral wave direction, c_x, and c_y are energy propagation speed in x and y directions, respectively, c_θ and c_ω are energy propagation speed in θ and ω domain, respectively, $\sigma = [gk \tanh (kd)]^{1/2}$ is the intrinsic frequency, g is the gravitational acceleration, k is wave num-

Table 5. *Summary of changes on breaking wave height modulation along the coast.*

Wave Dir.	T = 10s	12s	14s	16s	20s
ENE : M[1]	—[5]	—	—	0.5	0.38/1.33
: S[2]	—	—	0.6	0.64/1.22	0.69
: R[3]	NG[6]	0.9	1.38	0.83	0.86/1.33
: N[4]	0.5	NG	NG	0.83	NG
E : M	—	—	—	0.5/1.54	0.61/0.75
: S	—	—	0.88	0.7/1.14	0.94/1.72
: R	NG	NG	NG	1.2	1.27/1.2
: N	0.9	0.33	0.87	0.5	0.71
ESE : M	—	—	—	3.0	1.75/2.67
: S	—	—	NG	NG	1.22
: R	2.0	NG	NG	2.25	1.6/0.75
: N	NG	NG	2.25	2.0	NG
SE : M	—	—	—	1.12	NG
: S	—	—	1.33	1.28/1.16	1.55
: R	NG	1.83	1.5	1.5	2.0
: N	NG	0.46	2.0	1.55	NG

[1] : represents the Most Severe Sea wave condition.
[2] : represents Severe Sea wave condition.
[3] : represents Rough Sea wave condition.
[4] : represents Northeaster wave condition.
[5] : — denotes not included in computation.
[6] : NG denotes for negligible small.

ber, d is water depth, and S is the summation of energy source and sink terms representing the effects of wind energy input, S_i, bottom friction, S_f, white capping, S_c, breaking dissipation, S_b, as well as wave-wave interactions, S_w. Details of each source and sink terms are not presented here, but these are important items that affect the model performance.

SWAN model is solving Eq. 1 directly without any simplification. Because there are five dimensions (t, x, y, θ, and ω) to deal with, it is slow in computation. To speed up the computing speed, different degrees of parametricization or simplification were made. For example, HISWAP model uses parametricization on frequency domain, and thus, reduce to four dimensions (t, x, y, and θ). The STWAVE uses parametricization on frequency and direction domains and further assumes the steady state to obtain high computing speed. All the wave hindcast/prediction models also included some of the wave transformation processes (*e.g.,* shoaling, refraction, bottom friction) to improve accuracy at near coastal areas, but some of the processes (*e.g.,* diffraction, reflection) are hard to be included. Thus, these models are good for open coasts that do not have a complicated bathymetry, and wave reflection is negligible.

All models in this category also called "phase average" models because detailed wave phase information is not available and grid size can be relatively large, *e.g.,* on the order of ½ wave length. This is one of the advantages to use this kind of model for a large domain.

Models in the second category are designed to simulate wave transformation processes by solving the simplified mild slope equation (RADDER, 1979), the original mild slope equation (BERKHOFF *et al.,* 1982), or the extended mild slope equation (PORTER and STAZIKER, 1995; SUH *et al.,* 1997) given next. These models don't have the capability to simulate wave growth, white capping, and wave-wave interactions. Thus, the use of models in the second category is limited to the conditions in which wave growth is not important, *i.e.,* the wind is not strong or the study domain is not large enough to produce significant wave growth.

$$\nabla(CC_g\nabla(\phi)) + k^2CC_g(1 + if)\phi$$

$$+ [gf_1(\nabla^2h) + gkf_2((\nabla h)^2)]\phi = 0 \qquad (2)$$

where φ is the complex velocity potential function for wave field, ∇ stands for spatial gradient, C is the wave phase velocity, C_g is the group wave velocity, k is wave number, i is $(-1)^{1/2}$, f is a factor for all kind of wave energy loss, f_1 is a function of bottom curvature, ∇^2h, and f_2 is a function of bottom slope square, $(\nabla h)^2$. All models in this category also called "phase determined" models because detailed wave phase information can be calculated and wave direction can be calculated from the phase information. It requires, however, the grid size to be less than 1/7 of the wave length to have reasonable accuracy on wave phase. This is probably the drawback of using this kind of model because the computing domain cannot be large to have a reasonable computing speed.

Even in the second category, not all the models have the same capability (MAA *et al.,* 2000). For example, REF/DIF-1 (KIRBY and DALRYMPLE, 1991; 1994) solved the simplified mild slope equation with excellent computing efficiency but only work on monochromatic waves for weak diffraction and no wave reflection. On the other hand, RIDE solved the extended mild slope equation for all the five major wave transformation processes but at the cost of computing time. We chose the REF/DIF-1 over others for the following reasons:

1. The spectrum models used for wave prediction do not have the capability to simulate combined wave diffraction and refraction, which are the major effects that should be considered for this study.
2. When dealing with each component wave for open coasts without wave reflection nor strong wave diffraction, the REF/DIF-1 is an accurate wave transformation model for wave energy distribution.
3. The spectrum model that can simulate combined wave diffraction and refraction, *i.e.,* REF/DIF-S, actually ignores wave-wave interactions and runs REF/DIF-1 many times by considering the major contribution from the major direction, period, and wave heights with minor contributions from other frequencies, directions, and heights. Thus, the results are smoothed and better match the random waves. The results of a narrow-band wave spectrum transformation, however, should be approximately the same as that obtained from REF/DIF-1. This is because a narrow-band wave spectrum has limited contribution from other minor frequencies, directions, and heights. Thus, it can be reasonably represented by a single significant wave height and a single peak-energy wave period. For this reason, we selected using REF/DIF-1 to check the transformation process more clearly and efficiently. Instead of selecting only a few wave conditions, we selected 60 wave conditions, so we can see the differences between pre- and post dredging and between different wave conditions more clearly.
4. The concern of over/under prediction by using REF/DIF-1 is not necessary because we are dealing with each component of a wave spectrum. The random sea is better represented using a wave spectrum, but each component's behavior still can be modeled accurately using a monochromic wave model.

Calibration of REF/DIF-1

While using REF/DIF-1, a user may select to use (1) linear wave, Hedges weak non-linear (HEDGES, 1976), or Stokes' non-linear wave model; (2) select a bottom friction type of laminar, percolation, or turbulent wave boundary; and (3) select a pass-through or reflection lateral boundary conditions.

To address the first choice, we tried the three possible options by comparing computing results with the measurements at the near shore station MD001. The results from the second choice, *i.e.,* Hedges weak non-linear wave model, provided the closest match with observations, and thus, was used for all other computations.

To allow oblique incident waves (or normal incident waves which changed their direction while propagating toward the coast line) to pass-through the lateral boundary without reflection, the pass-through boundary condition was selected for all the studies. The lateral dimension on the computing grid was also selected to be large enough (67.56 km) to avoid

any influence by the possible imperfect boundary conditions in the numerical scheme.

It is well documented that bottom friction caused by turbulent wave boundary is the major source of energy loss (MAA and KIM, 1992). It is also documented that one should test a model by using different wave friction factors in order to match the predictions and observations (MAA and WANG, 1995). In summary, the reasons to conduct the calibration of a wave transformation model are (1) to make sure that the selected wave model can accurately simulate the wave transformation processes that are critical for the objective. Only through calibration, is it possible to know if the selected model has been set up properly. Any bug in the application of the selected computer model can be removed, assuring correct results. (2) Only when the wave model results are accurate, can the calculation of shoreline responses be meaningful. (3) Application of any model requires acceptance of many assumptions, including selecting a proper value for bottom friction. The calibration process provides the ability to apply rational, as opposed to arbitrary values. (4) Calibration is a form of quality control. Verification of a model's results against measurements builds confidence for others as to the modeling results.

In this study, we selected a month (Nov. 1–30, 1997, Figure 3) to calibrate the bottom friction coefficient. Wave measurements at Station 44009 were used as input wave conditions specified at the offshore boundary of the computing domain. Wave measurements at the near shore stations MD001 were selected to check the computing results. The coordinates of MD001 were translated to grid locations and wave heights calculated at all the nine neighboring grid points were averaged to compare with the measurements.

Even within one month, there are too many wave conditions to calculate if all the measured offshore wave conditions are used directly. For this reason, we sorted the wave conditions according to the specific intervals given before, and the number of wave conditions were reduced to 113 based on 10 different wave heights (5.0, 4.5, 4.0, 3.5, 3.0, 2.5, 2.0, 1.5, 1.0, and 0.5 m), six wave periods (4, 6, 8, 10, 12, and 14 s), and seven wave directions (NNE, NE, ENE, E, ESE, SE, and SSE). Using these 113 wave conditions, a time series of idealized wave conditions at the offshore boundary can be obtained (Figure 3a). Because waves that travel away from shore are excluded in this comparison, some data are excluded, and thus, the time series (marked as + in Figure 3a) is not a continuous line.

By trial and error, we found that a wave friction factor of 0.02 yielded the best match of the calculated and measured wave heights (Figure 3b). Considering that significant wave height is a widely accepted parameter to represent wave severity, the comparison given in Figure 3b shows that even a rather simple model (REF/DIF-1) performs well in wave height.

During the calibration period (Nov. 1–30, 1997), the maximum significant wave height at the offshore boundary was five meters. This is not large enough to include the possible most severe sea ($H_s = 8$ m), but is close to the severe sea condition ($H_s = 6$ m), thus, the calibration is considered sufficient and satisfactory.

WAVE TRANSFORMATION FOR THE ORIGINAL BATHYMETRY

In order to obtain a baseline for estimating the possible impact of sand mining at the two offshore shoals, wave transformations for the original bathymetry were performed first. Sixty possible wave conditions were selected to represent the majority of possible waves which can be affected by the potential sand mining.

Examples of the calculated wave height distributions in the display domain are shown in Figures 6 to 9. All other calculated distribution of wave height can be found in CUTTER *et al.* (2000). These figures use a gray scale to show the normalized wave height distribution, H/H_o (local wave height/incident wave height).

In general, large waves attenuated significantly because of the great energy dissipation caused by the large near-bed velocity. Large waves also may break on the shoals, as seen by the dark gray areas in Figures 6–9 (waves coming from two of the major directions, ENE and E). Notice that in the area between XG = 8 to 20 km and YG = 10 to 13 km, waves could be quite large if coming from east.

For the Northeaster and rough sea conditions ($H_s = 2$ and 4 m, T = 10–20 s), wave height distributions show mixed results toward the coast. Near the location mentioned above (XG = 8–20 km and YG = 10–13 km), which is south of Ocean City, waves from East tend to converge. The high wave energy (for all waves from the east) may be responsible for causing the shore line retreat at this area.

The relatively severe beach erosion south of Ocean City has been noticed for at least 100 years, long before constructing the jetties. After the construction of jetties at the Ocean City Inlet in 1930s, the severity increased because the jetties block the southward sediment transport, at least for many years before the by-pass system was implemented (SMITH, 1988).

Notice that near the Maryland-Delaware border (XG = 7–10 km, and YG = 24–28 km), the extensive wave height attenuation is obvious (the dark gray in Figures 6 to 9) which may be caused by wave shoaling and breaking after waves pass the Fenwick Shoal.

For a random sea that has many wave frequencies centered at a given frequency used in the REF/DIF-1 model, we may expect the wave height images shown in Figures 6 to 9 would be smoothed. The general trend, however, should be the same.

It should be noted that energy loss caused by bottom friction is not a linear process. This is because the energy loss is proportional to u_b^3, where u_b is the near bed velocity induced by waves. Figures 6 to 9 clearly show this nonlinear process. Local wave heights within the area between XG = 10–15 km and YG = 10–12 km are roughly 8 m, 7 m, 6 m, and 4 m, but the incident offshore wave heights are 8 m, 6 m, 4 m and 2 m. Wave period is 16 s and coming from the east for all the four cases.

If bottom friction is not considered, one may use a unit deepwater wave height, $H_o = 1$, to estimate local wave heights for all levels of sea severity. If including energy loss caused by bottom friction, the idea of using offshore unit wave height cannot be defended. This is the reason why four wave
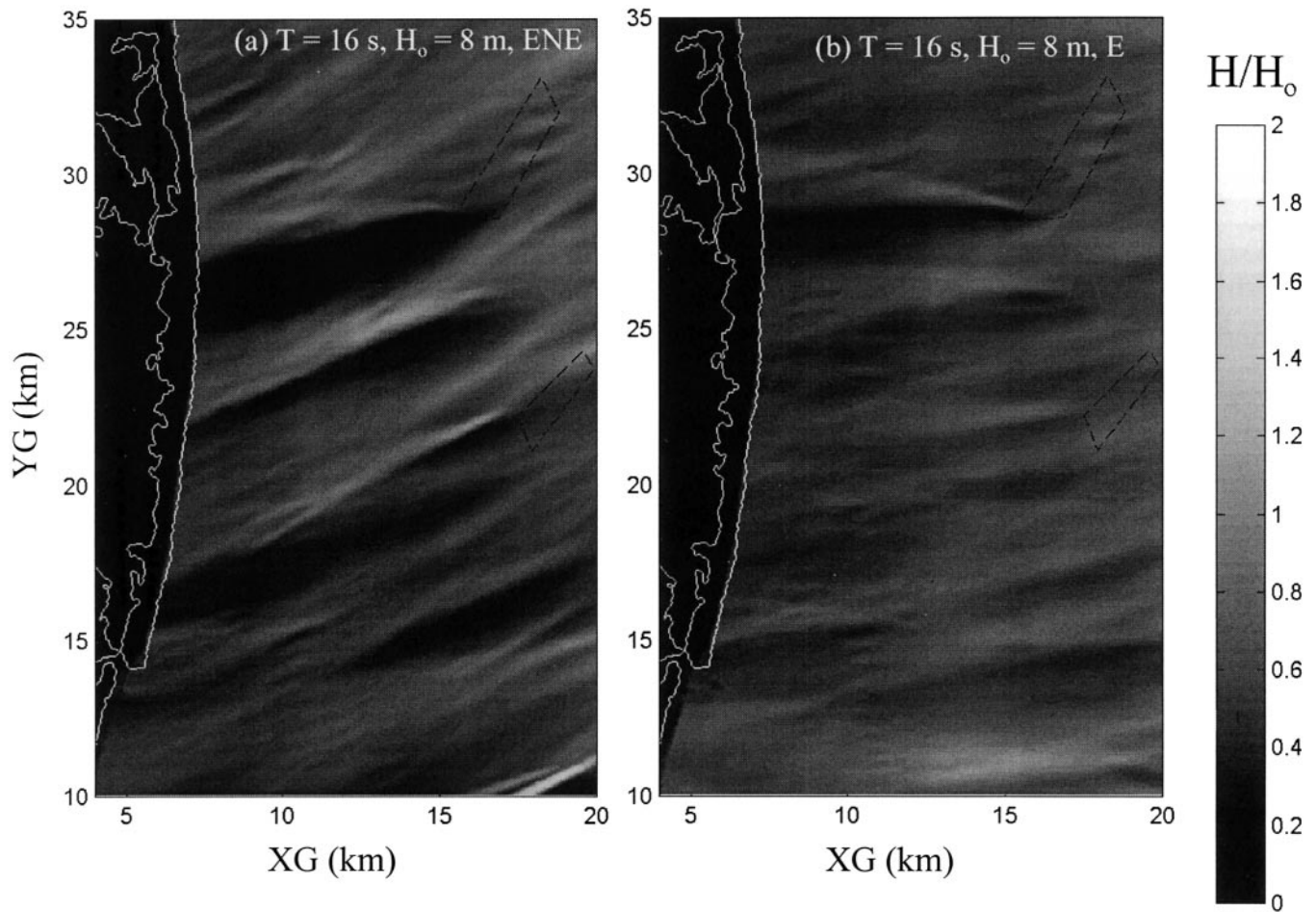
Figure 6. Normalized wave height distribution for the original bathymetry with $H_o = 8$ m and $T = 16$ s, and coming from (a) ENE, and (b) E. The planned dredging sites over Fenwick and Isle of Wight Shoals are marked by the dashed-dotted polygons.

heights were included in the study. It also implies that when simulating beach responses using all the reorganized wave heights and wave periods, one has to calculate hundreds of wave conditions.

CHANGES OF WAVES AFTER CUMULATIVE MINING

The dredging scenario is for a long term (10 to 20 years) sand mining event on the order of 24×10^6 m³. The objective is to assess the possible alteration of waves by sand mining at the two shoals. The same wave conditions that were used for checking the pre-mining wave height distribution were used again.

Sample plots of the normalized wave height difference (*i.e.,* $\Delta H/H$, in unit of %) are shown in Figures 10 and 11 to give a general idea of the difference in computed wave height between the offshore dredging sites and the coast. Comparison of other wave height differences can be found in CUTTER *et al.* (2000). Solid contours represent increase (*i.e.,* $\Delta H/H > 0\%$) and dashed contours represent decrease (*i.e.,* $\Delta H/H < 0\%$).

The modeled dredging areas are shown as the dashed-dotted polygons in these figures. It is important to point out that because the distance between these two dredging sites (Fenwick Shoal and Isle of Wight Shoal) is large, there is no interaction between the alterations to wave transformation. In other words, the possible impact caused by dredging at the modeled sites can be treated independently. Note that the severely affected ($\Delta H/H > 50\%$) areas are limited for large incident wave heights and the significantly affected area are limited on the north and south sides of the entire affected area, see the contours in Figure 10 for $H_o = 6$ m. When H_o is not significantly large, the difference is limited (*i.e.,* $\Delta H/H < 40\%$, see Figure 11). In the middle of these severely affected areas, wave heights are actually reduced ($\Delta H/H < 0\%$), indicated by the dashed contours. The most affected areas are between the shoreline and the dredging sites. At the dredging sites, there are only small differences in terms of wave height alteration.

The most significant difference is the great increase of wave height downstream of the south end portion of the Fen-
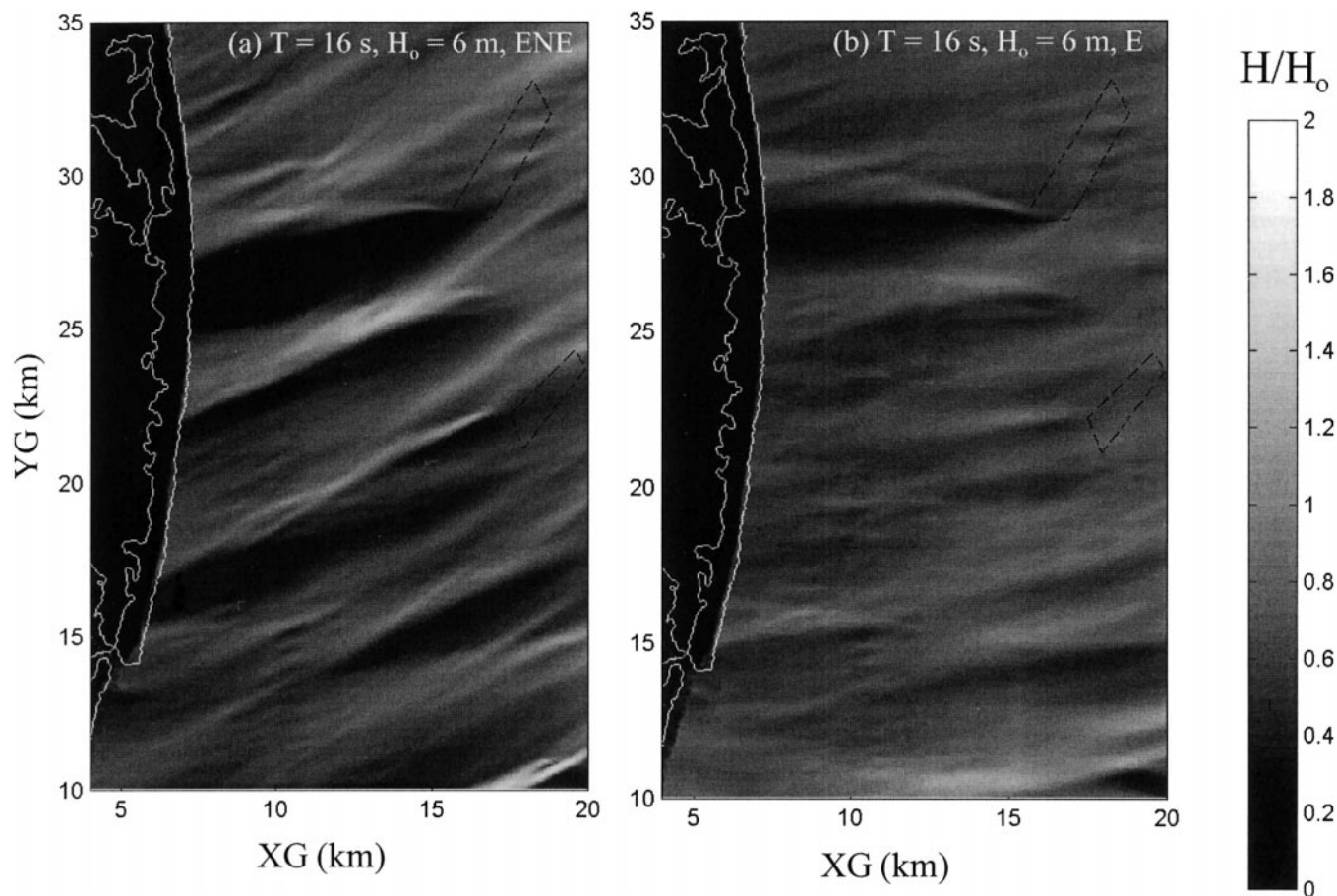
Figure 7.   Normalized wave height distribution for the original bathymetry with H_o = 6 m and T = 16 s and coming from (a) ENE and (b) E.

wick Shoal. For other affected areas wave height changes are either a moderate increase or decrease. The large increase of wave height is caused by the proposed dredging that increases the water depth to 9 m (original 6 m), and thus, no wave breaking attenuation at the south of the Fenwick shoal.

As far as the possible shoreline variations are concerned, we need to consider the change of breaking wave height along the shore. Here we suggest using the Breaking wave Height Modulation (BHM) as an index to examine the change of breaking wave condition (MAA *et al.,* 2001). BHM is actually the amplitude of breaking wave height along the coast. The larger the BHM, the more the local shoreline changes. If BHM = 0, it represents an ideal case that the shoreline will not change because the alongshore gradient of transport force is zero. The BHM at any location along the shore for the original bathymetry is assigned as 1 as a reference. The increase of BHM at any location indicates an increase of alongshore sediment transport at that location. On the other hand, a decrease of BHM represents the alongshore force gradient is reduced. Examples of the changes of breaking wave heights in the display domain are plotted in Figures 12 and 13. Comparison of all the breaking wave height profiles can be found in CUTTER *et al.* (2000).

We will use one specific case to explain the possible changes in details, and summarize the results in Table 5. For the most severe sea (Ho = 8 m, T = 20 s) coming from the ENE, Figure 12 indicates that the BHM increases a little (BHM = 1.33) between YG = 20 and 22 km, but the BHM has a significant decrease (BHM = 0.38) between YG = 25 to 27 km. If waves come from the E, the possible impact is positive (*i.e.,* BHM = 0.61 at YG = 30.5 km and 0.75 at YG = 19 km). For waves that come from the ESE, the results are all negative (BHM = 1.75 at YG = 30.5 km and BHM = 2.67 at YG = 23 km). If the waves come from SE, then there is almost no change.

When wave period decreases, the big difference in BHMs for waves coming from ENE at the Maryland and Delaware board diminishes. This is an indication that when considering the impact on wave transformation, more attention should be paid to long period waves.

The results on breaking wave height modulation are a mix of positive and negative (Table 5). Within the 60 studied wave conditions, 18 wave conditions do not show a measurable or significant change. Although for some waves that come from ESE there is a relatively large negative impact (*e.g.,* BHM > 2.), it is not a really significant negative impact because of
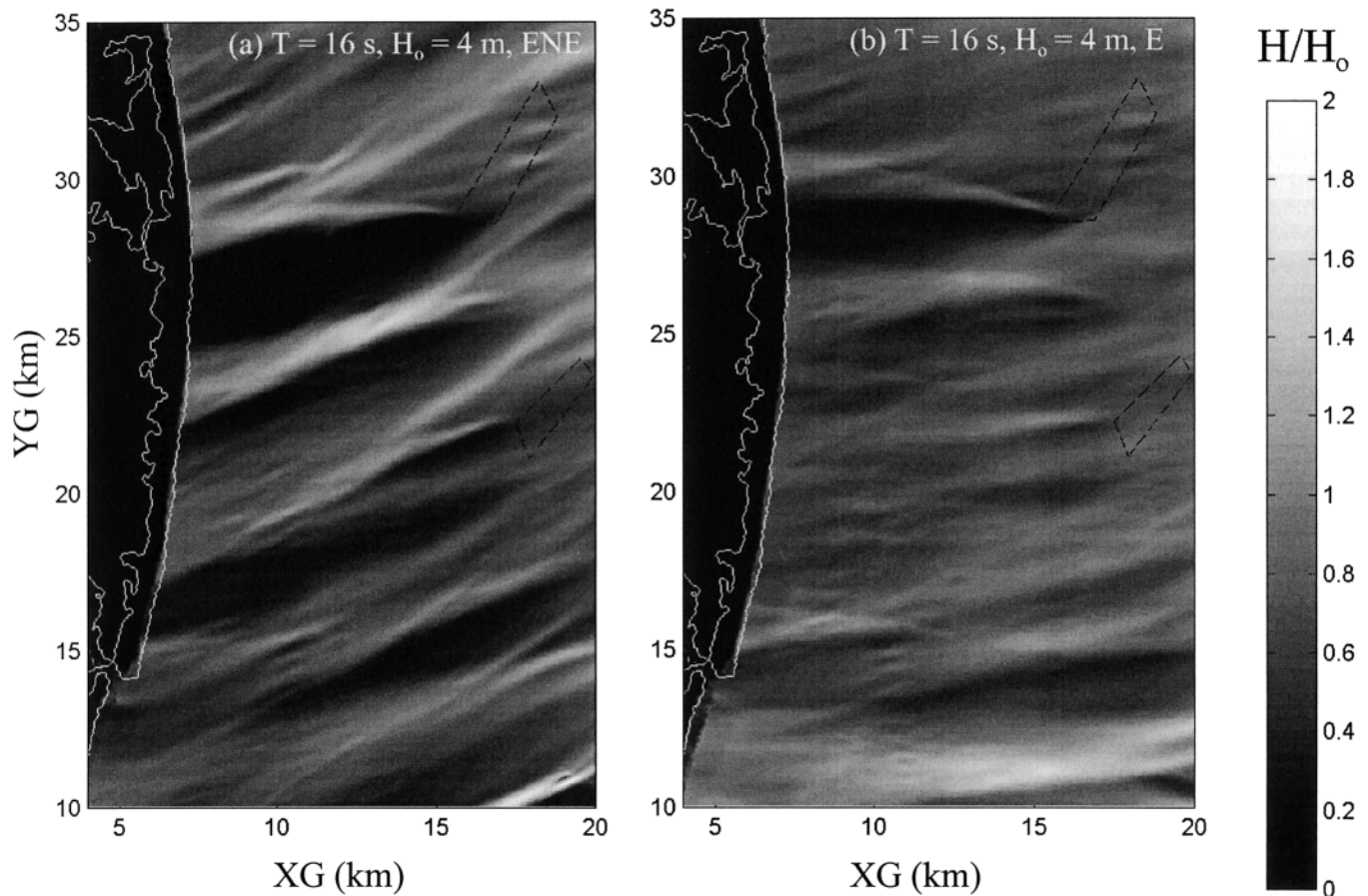
Figure 8. Normalized wave height distribution for the original bathymetry with $H_o = 4$ m and $T = 16$ s, and coming from (a) ENE and (b) E.

the originally small BHM. It is necessary to note that the numbers displayed in Table 5 are indices to show the relative significance. Absolute value of the change is another important information for making judgment. The most important feature in Figures 12 and 13 is the obvious reduction of BHM around YG = 26 km, the border between Maryland and Delaware. The original low breaking wave height means the sediment transport at this location is minimal. The obvious reduction of BHM (mainly for long period waves) actually increases the breaking wave height, and thus, indicates that the along shore sediment transport will move more sediment away from this location. Shoreline recession would be expected as a consequence. This is a negative impact at this particular location, however, the increased amount of sediment transport, moving either north or south, will benefit the downstream beaches. If sand resources are taken from the two shoals as modeled, some sort of beach protection project should be considered, or at least a monitoring project that closely checks the shoreline change at the Maryland and Delaware border should be established. If it is necessary to maintain the original shoreline, then part of the sand resources obtained from the offshore mining should be placed at this location.

POSSIBLE IMPACT ON TIDAL CURRENTS

The possible influence on tidal currents, especially the near bottom current, caused by the planned sand mining at the offshore shoals was studied using the three-dimensional (3-D) barotropic version of the Princeton Ocean Model (POM, BLUMBERG and MELLOR, 1987). As the POM is a well known model, the formulation part of this model is omitted, only the open boundary conditions, model verification, modeling results for the original tidal current distributions, and modeling results of the possible differences caused by sand mining are presented.

The orthogonal curvilinear model grid used for tidal current modeling is the same as that displayed in Figure 1, except that the cell size is increased to 300 m × 600 m in the east-west and north-south directions, respectively. The total dimensions also are the same: 44.97 km × 67.56 km. There are 6 sigma layers in the vertical direction, *i.e.,* the total water depth was divided into 6 layers. The thickness of these layers varies at each cell because of the different total water depths. The model computation internal and external time steps were 90 and 6 seconds, respectively. The horizontal diffusion coefficient was set as a constant of 50 m²/s.
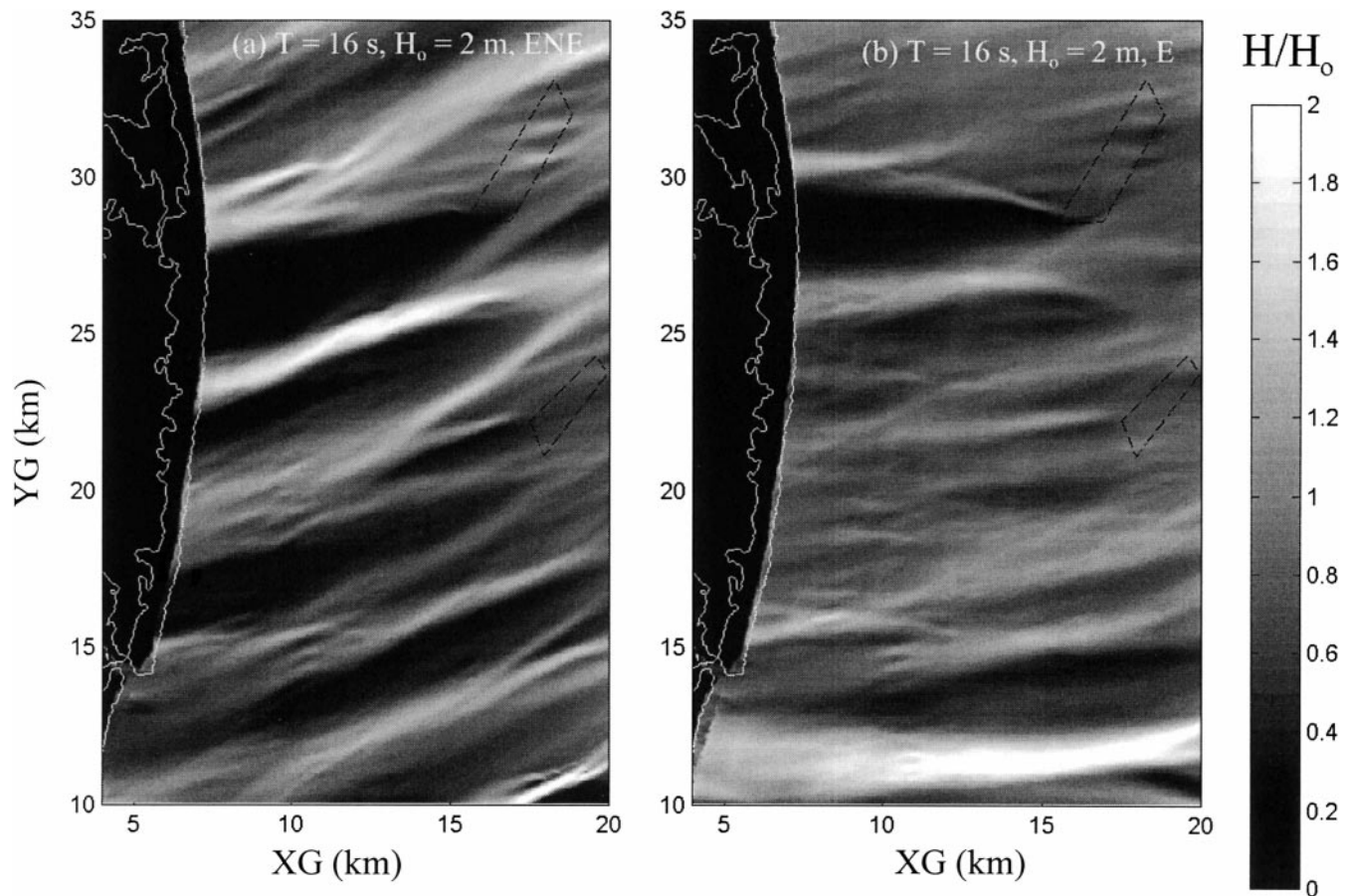
Figure 9.   Normalized wave height distribution for the original bathymetry with H_o = 2 m and T = 16 s, and coming from (a) ENE and (b) E.

Since tidal waves mainly propagate in the shore-normal direction at this study site, and the eastern open ocean boundary of the model domain is located only about 45 km offshore, the tidal level gradient is expected to be insignificant within this short distance. Therefore, the eastern open ocean boundary can be specified using the tidal levels measured from a tidal station on the west side of the study domain: Ocean City, Maryland. The only unknown is the phase angle required to produce a matched tidal time series at the Ocean City. To obtain the amplitudes of each tidal component, hourly water level records at Ocean City Inlet (NOS Station ID 8570283), Maryland for the entire year of 1985 were processed by using least square harmonic analysis for 29 tidal constituents. Using the 29 constituents, a tidal time series can be reconstructed to remove the wind effects: wind set-up or set-down. The reconstructed tide levels with a specified phase angle were specified as the east open ocean boundary condition while a velocity radiation condition was specified at the north and south boundaries. As mentioned before, the gradient of water surface elevation is negligibly small in this small domain, the reconstructed tidal elevations really serves three purposes: (1) to provide the boundary condition at the offshore border, (2) to serve as a base for finding

the correct phase angles that can be used at the east boundary of the computing domain, and (3) to verify the model performance by comparing the calculated and the reconstructed tidal elevation at the Ocean City Inlet.

Using the original bathymetry, the POM model was run with a cold start (assuming the tidal elevation and tidal current are all zero is the computation domain) for 30 "days." Comparison of the model calculated tide levels at Ocean City, Maryland with the re-constructed tide levels reveals very good agreement, less than 1 cm RMS (root-mean-square) error. This calibration indicates that the model is capable of reproducing the water levels accurately for the existing bathymetry in the study area. Although there is no tidal current information available to verify the simulated velocity, the model produces a reasonable (20 cm/s) maximum surface current speed at proposed dredging sites. Therefore, the model can be used to evaluate the tidal current changes before and after the proposed sand mining.

Contours of near-bed (bottom layer) tidal flow fields at the maximum flood and the maximum ebb, within the display domain (Figure 14) reveal that the near-bed tidal current is weak, less than 5 cm/s for the near shore (water depth < 10 m), except at the shoals, where the near-bed maximum flood
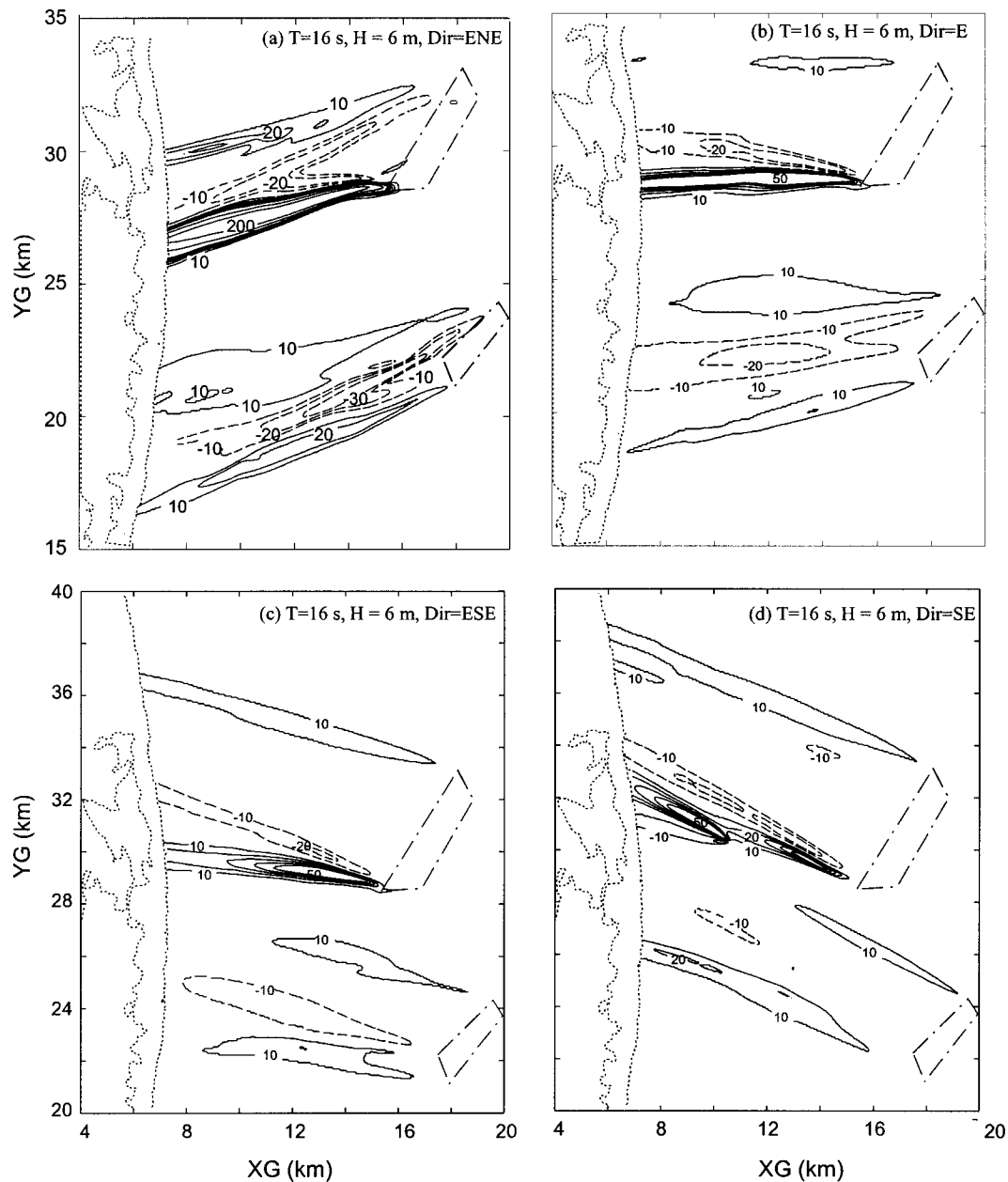
Figure 10.   Calculated changes of wave height (ΔH) normalized by the original wave height (H) for cumulative sand mining with H_o = 6 m and T = 16 s coming from (a) ENE, (b) E, (c) ESE, and (d) SE.

velocity is on the order of 8 cm/s. For the maximum ebb, the same conclusions also hold. Velocity vectors (Figure 15) within a small domain that includes Fenwick Shoal and Isle of Wight Shoal for the maximum flood and ebb reveal clearly the effect of bathymetry on tidal currents. When the tidal current is forced to flow over the shoal, the velocity increases because of the decreasing water depth. If the tidal current can find an easy way to avoid climbing the shoal, it will take the easy route.

Using the same offshore boundary condition, the same lateral boundary condition and the bathymetry with the cu-

mulative sand mining, the POM model was re-run to find the possible differences. For better visual presentation of the differences in such a small tidal current environment, we normalized the differences by presenting them in percentages (Figure 16) for the two extreme conditions: maximum flood and ebb. It clearly shows that a maximum difference on the order of 10% can result. In general, where the water depth increases because of dredging, the tidal current velocity decreases. Immediately downstream of the dredging site, and on the leeward side of tidal flow, tidal current velocity increases. The affected area is rather large, but the amount of
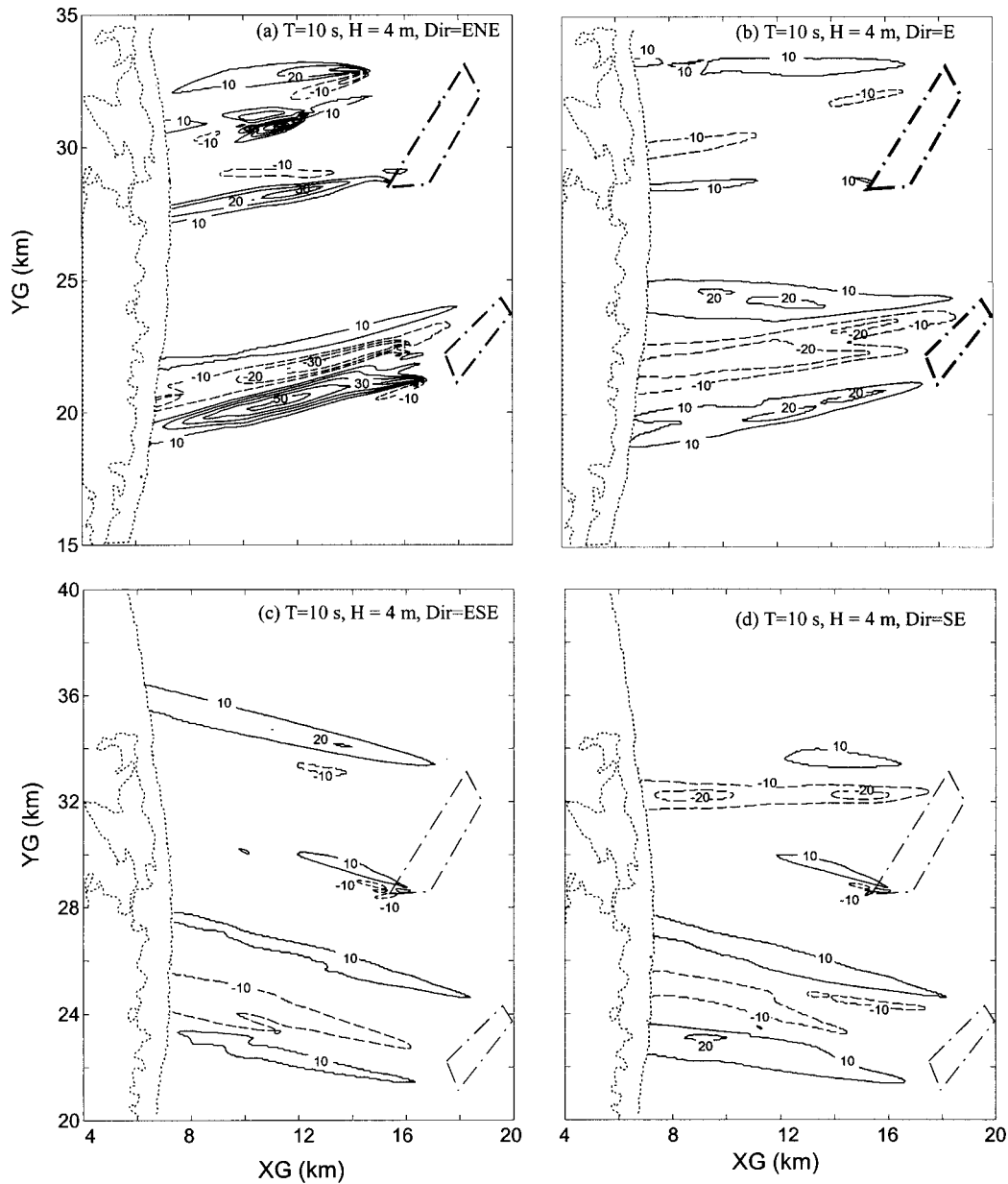
Figure 11.   Calculated changes of wave height (ΔH) normalized by the original wave height (H) for cumulative sand mining with H_o = 4 m and T = 10 s coming from (a) ENE, (b) E, (c) ESE, and (d) SE.

velocity increase is rather small, even as a percentage. If one considers that the maximum tidal current velocity is only around 8 cm/s at the shoal and around 5 cm/s away from the shoal, the change in tidal current caused by the proposed dredging should not affect biological living conditions.

POSSIBLE INFLUENCE ON STORM SURGE

Coastal storm surge, defined as the anomaly of water level from astronomical tide, is also known as wind tide because it stems from storms of tropical or extratropical origins. The storm surge has been expressed as barotropic response of coastal water body to meteorological forcing and the controlling parameters are geometry of coastlines and bathymetry (*e.g.* MURTY, 1984).

The SLOSH (Sea, Lake, and Overland Surges from Hurricanes) model (JELESNIANSKI *et al.,* 1992) was used in this study to assess possible changes resulting from the hypothetical sand mining. This model is the standard model used by NOAA to generate evacuation maps for Federal Emergency Management Agency. For this reason, details of this model are not given.

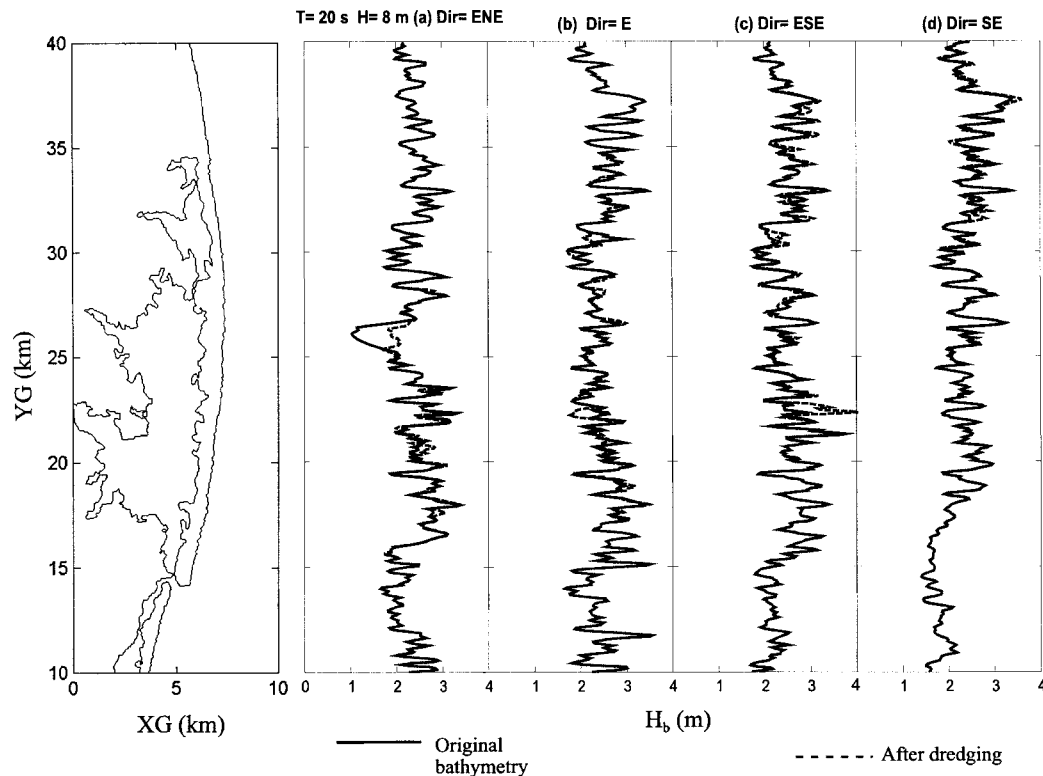A polar grid with 130 by 280 grid cells was constructed for

Figure 12. Comparison of breaking wave heights for original bathymetry and after cumulative sand mining with $H_o = 8$ m and $T = 20$ s.

this study. The coastal grid cells are approximately 150 m by 150 m. In order to investigate the impact from dredging of offshore sand shoals, we selected 10 stations along the coast to monitor the possible change of surges.

Tropical storms with an 86 mbar central pressure drop and 24-km maximum wind radius (comparable to category 4 storm) were used to simulate the coastal storm surges. Two orthogonal tracks of across-shore and along-shore directions were simulated. The results indicate that maximum surges were produced from the cross-shore track simulation (Figure 17). It clearly shows the higher coastal surges on the right hand side of the storm landfall points as would be expected. After re-run the SLOSH model with the post-mining bathymetry, the changes are about 0.1 cm that is negligible compared to the maximum surges of 3.5 m. Figure 18 shows the maximum surge from the along-shore track. In general, the coastal surges were lower compared to that generated from a cross-shore hurricane. South-north propagation of surges was evident, and the changes were also around 0.1 cm that again is negligible compared to the maximum surge of 2.5 m.

CONCLUSIONS

The possible impact on oceanographic parameters: wave transformation, tidal currents, and storm surge that might be caused by cumulative sand mining at Fenwick Shoal and Isle of Wight Shoal for a period of 10 to 20 years for a total of 2.4×10^7 m³ of sand are summarized as follows.

Using high quality raw bathymetric data, a computing domain of 44.970 km $\times$ 67.560 km was created for studying the possible changes on wave transformation and tidal currents. This grid is large enough to directly use wave data measured at an NOAA offshore wave station, 44009. The grid cell size, however, is small enough (30 m $\times$ 60 m) to show the effect of wave diffraction.

A total of 13 years of wave measurements from NDBC buoy station 44009, about 45 km offshore at the Ocean City, were used to analyze the possible choices of wave heights, periods, and directions that should be analyzed for alteration because of the modeled dredging at the two shoals. Two near shore wave stations, MD001 and MD002, provide about 4 years measurements. The measured waves at these two near shore stations are almost identical. Data from both the offshore and near shore stations provide a complete set for verifying the selected wave transformation model.

Sixty wave conditions are selected as model wave conditions. These wave conditions include four possible wave heights (2 m, 4 m, 6 m, and 8 m), five wave periods (10 s, 12 s, 14 s, 16 s, and 20 s), and four wave directions (ENE, E, ESE, SE). As wave energy loss caused by bottom friction is not a linear process, all four wave heights have to be included in the calculations. REF/DIF-1 was selected because of its excellent accuracy and computing efficiency. The model was calibrated using one-month of wave measurements (Nov. 1 to 30, 1997) from stations 44009 and MD001.
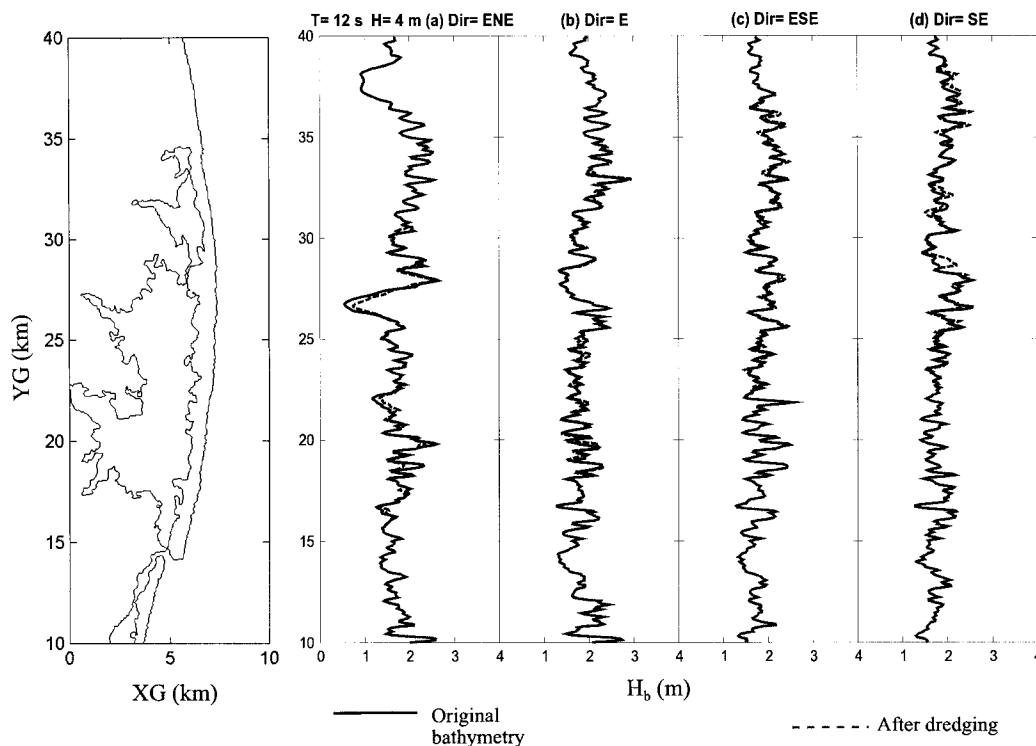
Figure 13. Comparison of breaking wave heights for original bathymetry and after cumulative sand mining with H_o = 4 m and T = 12 s.

The calculated wave height distributions for the original bathymetry indicate that just south of Ocean City, waves coming from East have a tendency to converge. The high wave energy (for all waves that come from East) may be responsible for causing the shoreline retreat south of Ocean

City. Near the Maryland–Delaware border, there is an area of extensive wave height attenuation due to wave shoaling and breaking after waves pass Fenwick Shoal that is approximately 10 km offshore. The relatively small breaking wave
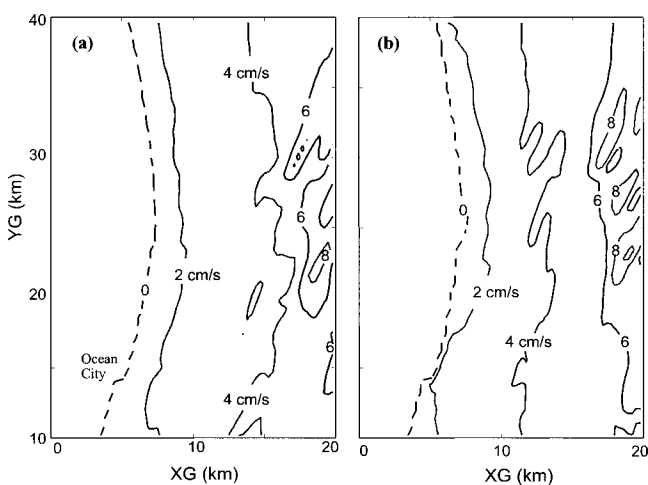
Figure 14. POM calculated contours of near-bed tidal current velocity (in cm/s) for a selected domain including Fenwick and Isle of Wight Shoals. (a) At maximum flood; (b) At maximum ebb. Zero contour line for tidal current is also the shoreline.
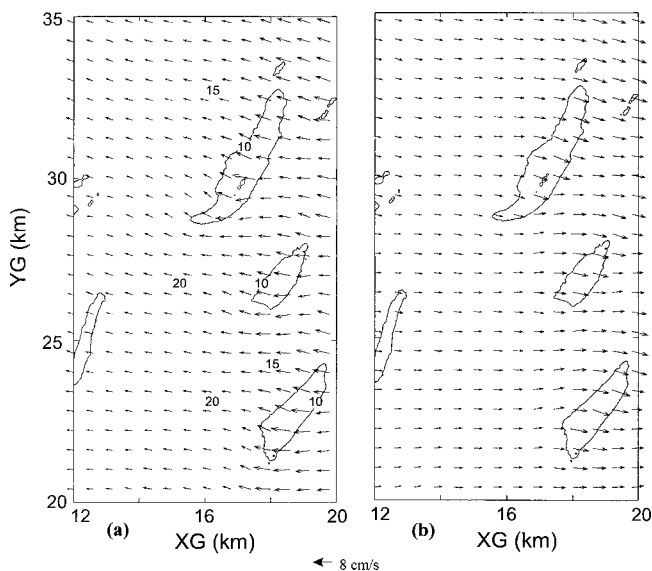

Figure 15. POM calculated near-bed tidal current velocity vectors for the selected domain at (a) maximum flood and (b) maximum ebb.
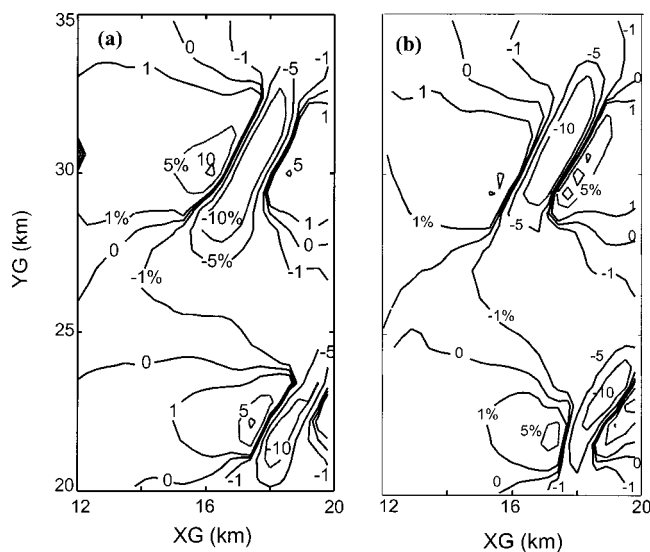
Figure 16. Difference (in %) in tidal current caused by sand mining at the modeled sites for (a) maximum flood and (b) maximum ebb.
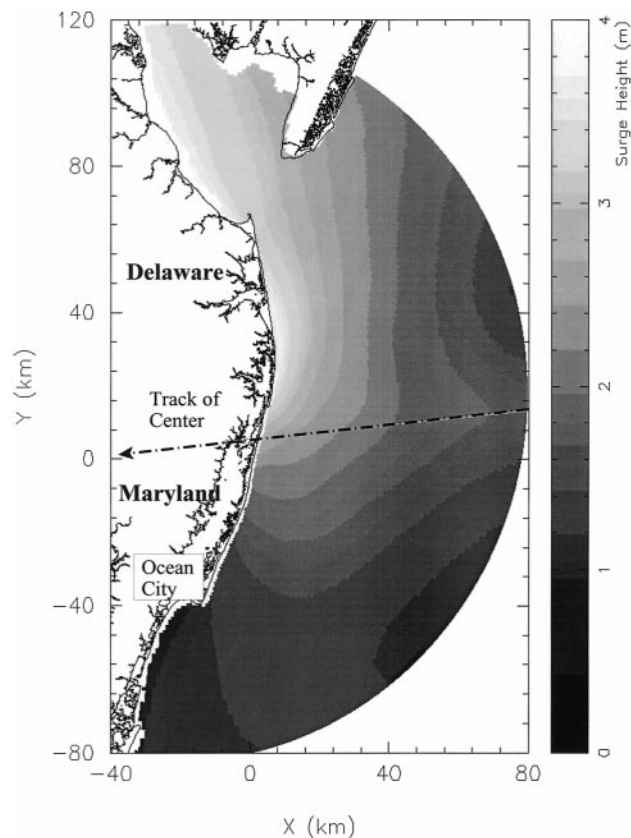

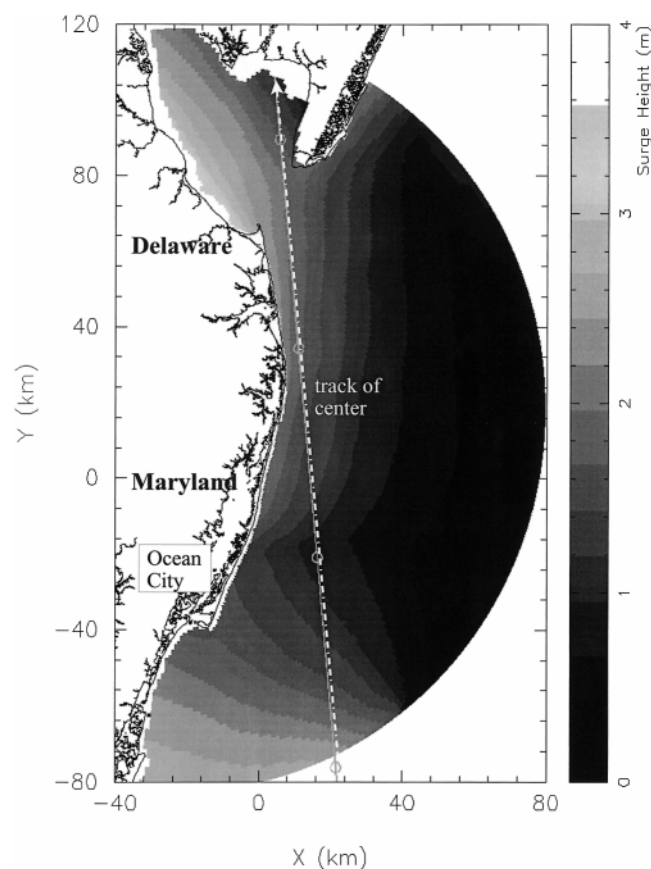Figure 18. SLOSH model calculated maximum storm surge for a category 4 storm that moves parallel to the shore.

Figure 17. SLOSH model calculated maximum storm surge for a category 4 storm that moves across the shore.

heights at this area may explain the relatively stable shoreline near the border.

This study indicates that the major change of wave height caused by cumulative sand mining at Fenwick and Isle of Wight Shoals is between the dredging site and the shoreline. The increase of local wave height can be as much as two times. The change of breaking wave height, on the other hand, is not so obvious except for the clear reduction of breaking wave height modulation (BHM) at the Maryland and Delaware border. The reduction of BHM at this location, however, is not necessarily a positive impact because it increases the breaking wave height at that location. As a consequence, more erosion and shoreline recession at that location might occur. Otherwise, the possible impact is not significant.

The SLOSH model with a category 4 storm that moves across the shore demonstrated that the possible change of storm surge caused by the modeled mining is only 0.1 cm which is negligible compared to the maximum surge of around 3 m.

The maximum near-bed tidal current is weak, on the order of 5 cm/s except at the shoals, where current velocity increases to around 8 cm/s. The postulated dredging at the shoals will reduce the maximum near-bed tidal current velocity (around 10%, *i.e.,* 1 cm/s). Immediately on the leeward side

of tidal flow, the dredging increases the tidal velocity, up to 10%. These results indicate a negligible impact. For future studies, the possible impact on current and storm surge may be excluded.

ACKNOWLEDGMENTS

LITERATURE CITED

BERKHOFF, J.C.W.; BOOIJ, N., and RADDER, A.C., 1982. Verification of numerical wave propagation models for simple harmonic linear water waves. *Coastal Engrg.,* 6: 255–279.

BLUMBERG, A.F. and MELLOR, G.F., 1987. A description of a three-dimensional coastal ocean circulation model. *In: Three-dimensional Coastal Ocean Models,* Coastal and Estuarine Science, Vol. 4 (HEAPS, N.S. ed.), American Geophysical Union, Washington, D.C., 1–16.

CUTTER, JR. G.R.; DIAZ, R.J.; MUSICK, J.A.; OLNEY, J.; BILKOVIC, D.M.; MAA, J.P.-Y.; KIM, S.C.; HARDAWAY, C.S.; MILLIGAN, D.A.; BRINDLEY, R., and HOBBS, III C.H., 2000. *Environmental Survey of Potential Sand Resource Sites Offshore Delaware and Maryland, Final Report OCS Study* 2000-055, Prepared for Minerals Management Service, U.S. Dept. of the Interior, Virginia Institute of Marine Science, Gloucester Point, VA.

HEDGES, T.S., 1976. An empirical modification to linear wave theory, *Proc. Inst. Civil Engrg.,* 61(2), 575–579.

HOBBS, III, C.H., 2002. An investigation of potential consequences of marine mining in shallow water: An example from the middle Atlantic coast of the United States. *Journal of Coastal Research,* 18(1), 94–101.

JELESNIANSKI, C. P.; CHEN, J., and SHAFFER, W. A., 1992. *SLOSH: Sea, Lake, and Overland Surges from Hurricanes.* NOAA Technical Report NWS 48, Department of Commerce, USA, 71p.

KIRBY, J. T. and DALRYMPLE, R. A., 1991. *User's Manual, Combined Refraction/Diffraction Model, REF/DIR 1,* Version 2.3. Center for Applied Coastal Research, Department of Civil Engineering, University of Delaware, Newark, DE 19716.

KIRBY, J. T. and DALRYMPLE, R. A., 1994. *Combined refraction/diffraction model REF/DIF-1,* version 2.5, documentation and user's manual. CACR Report 94-22, Center for Applied Coastal Research, University of Delaware, Newark, Delaware, 171p.

MEINDL, E.A. and HAMILTON, G.D., 1992. Programs of the National Data Buoy Center. *Bulletin of the Amerian Meterorological Society,* 73(7), 985–993.

MAA, J. P.-Y.; HOBBS, III C. H., and HARDAWAY, JR. C. S., 2001. A criterion for determining the impact on shorelines caused by altering wave transformation, *Journal of Coastal Research,* 17(1), 107–113.

MAA, J. P.-Y. and HOBBS, III C.H., 1998. Physical impact of waves on adjacent coasts resulting from dredging at Sandbridge Shoal, VA, *Journal of Coastal Research,* 14(2), 525–536.

MAA, J. P.-Y.; HSU, T.-W.; TSAI, C.-H., and JUANG, W. J., 2000. Comparison of wave refraction and diffraction models. *Journal of Coastal Research,* 16(4), 1073–1082.

MAA, J. P.-Y. and WANG, D. W-C., 1995. Wave transformation near Virginia coast: the 1991 Halloween Northeaster, *Journal of Coastal Research,* 11(4), 1258–1271.

MAA, J. P.-Y. and KIM, C.-S., 1992. The effect of bottom fiction on breaking waves using RCPWAVE model. *Journal Waterway, Port, Coastal and Ocean Engineering,* 118(4), 387–400.

MURTY, T. S., 1984, Storm surges-meteorological ocean tides, *Canadian Bulletin of Fisheries and Aquatic Sciences,* 212, 897p.

PORTER, D. and STAZIKER, D.J., 1995. Extensions of the mild-slope equation. *Journal Fluid Mechanics,* 300, 367–382.

RADDER, A.C., 1979. On the parabolic equation method for water wave propagation. *Journal Fluid Mechanics,* 95(1), 159–176.

SMITH, E. R., 1988. *Case Histories of Corps Breakwater and Jetty Structures,* Technical Report REMR-CO-3. Coastal Engineering Research Center, Dept. of the Army, Waterways Experiment Station, Corps of Engineers, Vicksburg, Mississippi, 133p.

SUH, K.D.; LEE, C., and PARK, W.S., 1997. Time-dependent equations for wave propagation on rapidly varying topography. *Coastal Engineering,* 32, 91–117.